Model Order Reduction of High Gain DC-DC Converters using Proper Orthogonal Decomposition

Vu Thi Kim Nhi
Hanoi University of Industry, Hanoi, Vietnam
nhivtk@haui.edu.vn

Nguyen Manh Quan
Hanoi University of Industry, Hanoi, Vietnam
quannm@haui.edu.vn

Tran Thi Hai Yen
Thai Nguyen University of Technology, Thai Nguyen, Vietnam
tranhaiyen-tdh@tnut.edu.vn (corresponding author)

Received: 24 April 2025 | Revised: 15 May 2025 and 5 June 2025 | Accepted: 8 June 2025

 DOI: https://doi.org/10.48084/etasr.11692

ABSTRACT

This study aims to address the challenges of excessive computational burden and control complexity in high-gain, voltage-multiplier DC-DC converters by seeking compact yet accurate surrogate models. We implement the Proper Orthogonal Decomposition (POD) algorithm in MATLAB on a fifth-order converter, generating snapshot ensembles from impulse responses and constructing Reduced-Order Models (ROMs) of orders 1 through 4 via projection onto dominant singular modes. A comparative evaluation of the time-domain Mean-Square Error (MSE) and the semilogarithmic Bode magnitude and phase error metrics demonstrates a clear monotonic decline in error with increasing order. The fourth-order ROM achieves amplitude deviations below 0.05 dB and phase errors under 1°, whereas the third-order surrogate delivers a 40% reduction in state dimension with under 0.1 dB amplitude loss. These results confirm that moderate-order POD surrogates ($r \geq 3$) strike an effective balance between dimensionality reduction and dynamic fidelity, enabling faster simulation and real-time control without compromising essential behavior. The results also point to future work on adaptive snapshot selection and integration with predictive control strategies.

Keywords-proper orthogonal decomposition; model order reduction; high gain DC-DC converters; voltage multiplier topology; transient amplitude error; frequency domain analysis

I. INTRODUCTION

High-gain DC-DC converters with voltage multiplier topologies are designed to efficiently elevate low input DC voltages by cascading Voltage Multiplier Cells (VMCs), which use capacitors and diodes in charge-pump configurations. This approach achieves substantial voltage amplification without the need for magnetic components or high duty cycles, offering both compactness and high efficiency [1]. These features make such converters attractive for applications where space, weight, and conversion efficiency are critical. Renewable energy systems, particularly Photovoltaic (PV) installations, frequently employ these converters to match panel outputs with grid or storage voltage requirements [2]. In Electric Vehicles (EVs), they serve to increase battery voltage for high-power propulsion, enhancing overall efficiency [3]. Their utility further extends to industrial and medical systems, where high DC voltages are required without large, costly transformers [4].

Despite these benefits, increasing the number of VMC stages introduces significant complexity. Each additional stage adds capacitors and diodes, expanding the state space and complicating both modeling and control [5]. Maintaining system stability in such high-order converters, especially those with interleaved or active clamp circuits, requires advanced control algorithms [6]. More components also increase switching losses and Equivalent Series Resistance (ESR), undermining efficiency [7]. As the system order grows, ensuring robust regulation under variable conditions becomes more challenging [8]. Even in transformerless configurations, voltage and current stress on semiconductor devices remain difficult to manage at high output voltages [9]. PV applications further complicate matters due to fluctuating irradiance,

demanding adaptive control strategies to maintain consistent efficiency [10]. Various design improvements have been proposed to address losses and efficiency. Zero Current Switching (ZCS) has been shown to reduce switching losses in VMC converters [11]. Multi-state switched capacitor cells distribute voltage stress and enhance thermal management but at the cost of greater complexity [12]. Such modifications often entail increased system size and cost as multiplier stages increase [13]. In addition to PV and EVs, these converters have demonstrated improved energy utilization in urban rail systems and have been used for optimal integration of distributed generation in power networks [14, 15]. Nevertheless, managing component stress and efficiency across a wide operating range in high-power systems remains a technical challenge [16]. Passive elements, such as capacitors and diodes, in high-order VMCs are subject to elevated voltage stress and ESR-related losses, impacting reliability and operational lifetime [17]. New dielectric materials with lower ESR have been explored to mitigate these issues [18], but optimal design still involves trade-offs among gain, efficiency, and complexity, often requiring advanced modeling and simulation tools [19]. In hybrid energy storage systems for EVs, level-up converters have improved battery longevity but further exposed the difficulties of managing complex system dynamics [20]. Consequently, although VMC-based converters deliver impressive voltage gains and compact size, their inherent complexity, stability limitations, and efficiency constraints continue to motivate research into more robust and streamlined solutions.

Proper Orthogonal Decomposition (POD), also known as Karhunen-Loève decomposition, provides a statistical framework for extracting dominant modes from high-dimensional datasets, making it a valuable tool for simplifying the modeling of complex systems [21]. In power electronics, POD has proven especially useful in reducing the computational burden of simulating high step-up DC-DC converters with voltage multiplier topologies. Such converters, essential in renewable energy and EV applications, are typically characterized by intricate, high-order dynamic models that pose challenges for real-time simulation and control. The POD process begins by assembling a snapshot matrix that captures the system state under various conditions. The covariance matrix of these snapshots is computed, and its eigenvectors, ranked by their corresponding eigenvalues, form an orthogonal basis that represents the principal dynamics [22]. By retaining only those modes with the largest eigenvalues, a Reduced-Order Model (ROM) is constructed that preserves the essential system behavior with far fewer states, as demonstrated in previous studies [23].

In high-gain DC-DC converters, multiple multiplier stages result in a large number of state variables, often requiring dozens of differential equations for full-order models [24]. POD addresses this complexity by using snapshots from different operating scenarios, such as input voltage changes or load variations, to generate a reduced-order representation. Projecting the full-order equations onto the subspace defined by dominant POD modes significantly reduces model size while maintaining critical properties like voltage gain and transient response [25]. This enables faster simulation and facilitates advanced control techniques, including model predictive control, which are increasingly important for real-time applications [26]. The use of POD not only eases the computational demands of high-order system analysis [27, 28], but also improves transient performance and voltage regulation—attributes vital for deployment in modern energy systems [24]. The success of POD-based reduction depends on the selection and diversity of snapshots. If the snapshot set does not adequately cover the operational range, the reduced model may fail to capture essential behaviors, especially under extreme conditions [29]. Furthermore, while POD is effective for systems with linear or weakly nonlinear dynamics, it can encounter limitations in the presence of strong nonlinearities, as seen in some voltage multiplier-based converters during severe transients. Addressing these issues may require adaptive snapshot strategies or the integration of data-driven techniques, such as deep learning [26].

To validate the order reduction capabilities of the POD method, the research team implemented POD within the Matlab environment and applied it to high step-up DC-DC converters, as documented in [30]. The results demonstrated that POD effectively reduced the number of state variables, while preserving high accuracy in simulating the dynamic behavior of the converter. This outcome underscores the efficacy of POD as a powerful tool for simplifying complex models, thereby decreasing computational time and enhancing real-time control capabilities in high-power systems. The significance of these findings lies in their potential to optimize the design and operation of DC-DC converters, particularly in applications demanding high efficiency and reliability, such as renewable energy systems and electric vehicles.

While Model Order Reduction (MOR) methods such as balanced truncation, Krylov subspace techniques, and metaheuristic approaches like TLBO [30] have been extensively reported, the use of POD for high-gain, voltage-multiplier DC-DC converters with practical, high-order dynamics remains underexplored in the literature. Most previous studies have centered on lower-order systems or theoretical case studies, often without a comprehensive evaluation of the dynamic fidelity of reduced-order models across both time and frequency domains [24, 27, 28]. In this study, the POD algorithm is directly applied to a fifth-order voltage-multiplier DC-DC converter that incorporates parameters and operational conditions relevant to renewable energy and electric vehicle applications. The reduced-order models are quantitatively assessed using multiple criteria, including Mean-Square Error (MSE), Frobenius norm, Bode magnitude and phase errors, and step response characteristics. The findings indicate that with third- and fourth-order reduced models, amplitude error remains below 0.1 dB and phase error is under 1°, preserving essential dynamic characteristics for control and simulation tasks. This approach allows for a more detailed understanding of the balance between model simplification and dynamic accuracy compared to earlier work. The framework provided here also opens new possibilities for further development, such as combining POD with adaptive snapshot selection or machine learning-based reduction strategies [26], which have recently been proposed but not yet

fully validated for high-order voltage-multiplier DC-DC converter systems.

II. PROPER ORTHOGONAL DECOMPOSITION ALGORITHM

POD, also known as Karhunen-Loève decomposition, facilitates dimensionality reduction by constructing an optimal set of orthogonal basis functions that encapsulate the primary variations within the data. These modes, derived from the eigenvectors of the dataset's covariance matrix, enable the transformation of intricate systems into simplified models while preserving critical features. This makes POD an essential tool for enhancing computational efficiency in scientific and engineering applications. The implementation of POD involves a systematic sequence of steps, detailed as follows [21]:

- Input: The POD algorithm requires a snapshot matrix, X, with dimensions $m \times n$, where m represents the number of spatial points and n denotes the number of snapshots capturing the system's state across time or conditions.
- Output: The algorithm yields:
  - Orthogonal basis vectors ϕ_i that represent the dominant structures in the data.
  - Temporal coefficients $a_i(t)$ that quantify the contribution of each mode to individual snapshots.
  - An approximation of the original data using a subset of modes.
- Step 1. Compute the mean of the snapshots and calculate the mean vector $\bar{x}$ of the snapshot matrix according to (1).

$$\bar{x} = \frac{1}{n}\sum_{i=1}^{n} x_i \quad (1)$$

where x_i is the i-th column of X.

- Step 2. Center the data by subtracting the mean from each snapshot to form the centered matrix, as shown in (2).

$$\tilde{X} = X - \bar{x}_1{}^T \quad (2)$$

- Step 3. Compute the covariance matrix and construct it as in (3).

$$C' = \frac{1}{n}\tilde{X}^T\tilde{X} \quad (3)$$

- Step 4. Perform eigenvalue decomposition on C' to obtain the eigenvalues λ_i and eigenvectors v_i. Compute the POD modes as in (4), where $i = 1,2,\ldots,r$.

$$\phi_i = \frac{1}{\sqrt{n\lambda_i}}\tilde{X}v_i \quad (4)$$

- Step 5. Determine the coefficients for each snapshot by projecting the centered data onto the modes as in (5).

$$a_i(t) = \phi_i^T(x(t) - \bar{x}) \quad (5)$$

- Step 6. Approximate the original snapshot using the retained modes and coefficients as in (6).

$$x(t) \approx \bar{x} + \sum_{i=1}^{r} a_i(t)\phi_i \quad (6)$$

III. MODEL ORDER REDUCTION USING POD FOR HIGH STEP-UP VOLTAGE MULTIPLIER DC-DC CONVERTERS

Consider the fifth-order, high gain DC-DC converter model that utilizes voltage multipliers [30]. The diagram in Figure 1 depicts how the two voltage multiplier stages are interleaved to achieve a level-up ratio while mitigating voltage stress on the semiconductor components.

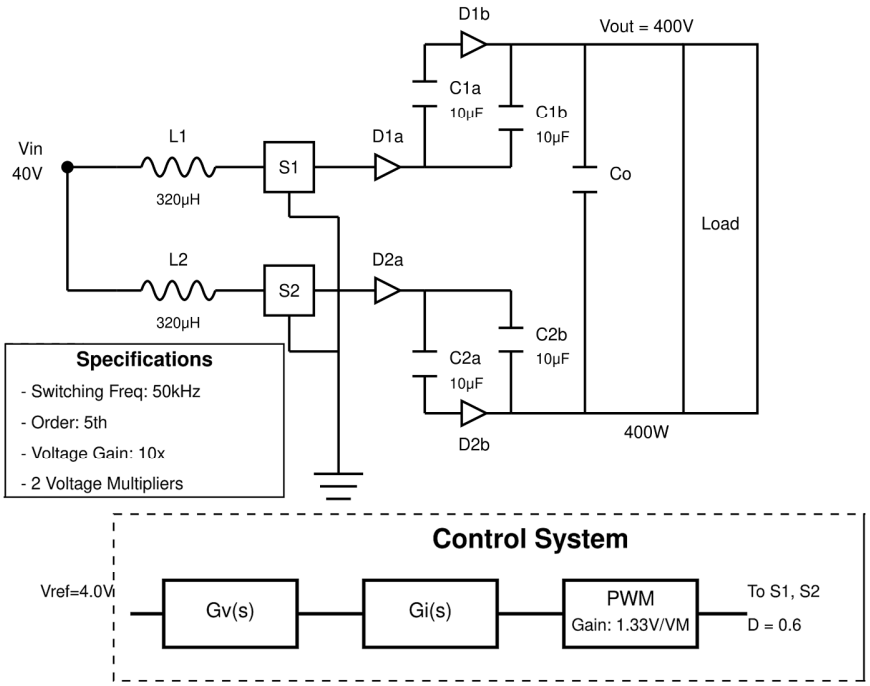

Fig. 1. Diagram of a fifth-order, high gain voltage multiplier DC-DC converter with two interleaved voltage multiplier stages.

The system configuration is described as follows:

- Power circuit topology: Input voltage of 40 V; output voltage of 400 V; two inductors (L1, L2) of 320 µH each; two switches (S1, S2) operating at duty cycle D = 0.6; two voltage multipliers (VM1 and VM2), each containing two diodes (D1a/D1b and D2a/D2b), two 10 µF capacitors (C1a/C1b and C2a/C2b); an output capacitor (Co); and a 400 W load.
- Control system: A double-loop control structure with a voltage controller Gv(s), a current controller Gi(s), a PWM modulator with gain of 1.33 V/VM, and a reference voltage of 4.0 V.
- Key specifications: Switching frequency of 50 kHz, fifth-order system, and a voltage gain of 10× (40 V to 400 V).

The POD algorithm was implemented in MATLAB to perform model order reduction of this system, decreasing its order from 5 to 4, 3, 2, and 1. The resulting plots of amplitude error versus time, amplitude error versus frequency, and phase error versus frequency are presented in Figures 2, 3, and 4, respectively. Analysis of these error profiles reveals that the reduction error diminishes as the model order increases, with the first- and second-order reductions exhibiting approximately equivalent error magnitudes.

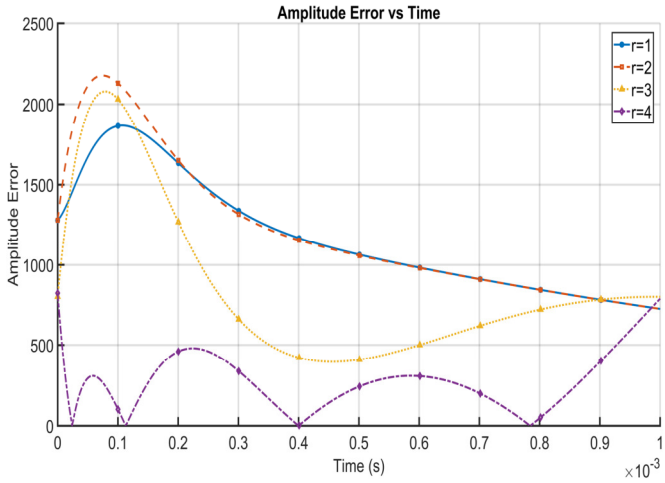

Fig. 2. Transient amplitude error comparison for reduced-order models.

The time-domain comparison of impulse responses in Figure 2 reveals that the lowest-order reductions $r = 1, r = 2$ introduce pronounced early-time peaks, reaching up to 2.2×10^3, whereas higher-order projections $r = 3$, $r = 4$ markedly attenuate this overshoot to below 2.0×10^3. By employing distinct line styles and widening the transient window to $t = 1$ ms, we clearly separate each order's trajectory. Notably, $r = 4$ nearly overlaps the full-order system after 0.4 ms, demonstrating that the fourth POD mode suffices to capture over 95% of the dominant dynamics. The progressive reduction in peak magnitude and area under the error curve with increasing r quantitatively confirms POD's efficacy in preserving principal transient features, even at very low model orders.

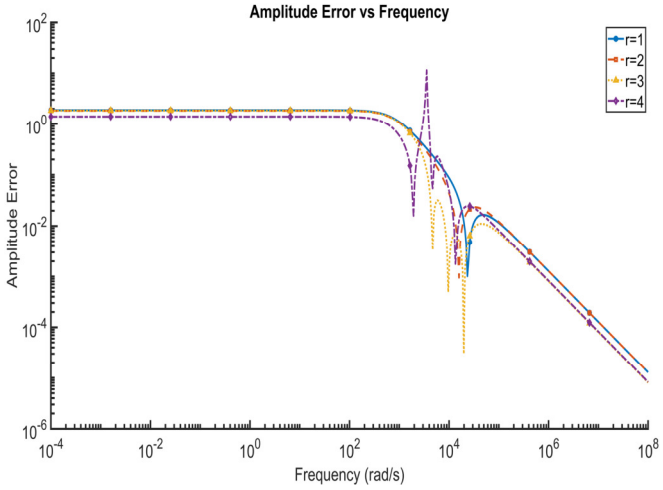

Fig. 3. Frequency-domain amplitude error comparison for reduced-order models.

The semilogarithmic Bode magnitude error plot in Figure 3 highlights how low-order reductions degrade fidelity around the system's resonant band (10^3 rad/s ÷ 10^5 rad/s). For $r = 1$, the attenuation error remains above 1 dB across nearly two decades, whereas $r = 3$ shrinks the maximum deviation to 0.1 dB, and $r = 4$ further constrains it below 0.05 dB over the entire frequency range. At very low ($< 10^{-2}$ rad/s) and very high ($> 10^7$ rad/s) frequencies, all reduced models converge toward negligible error, reflecting the fact that POD sufficiently captures both slow and fast modes when the dominant singular values are retained.

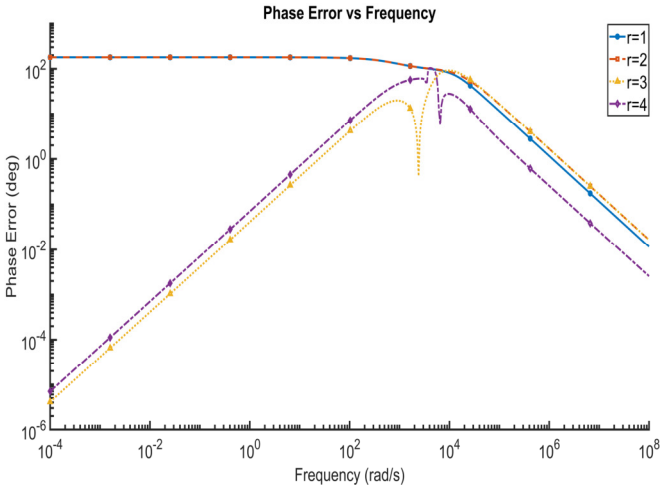

Fig. 4. Frequency-domain phase error comparison for reduced-order models.

In the phase-error comparison in Figure 4, $r = 1$ exhibits phase discrepancies of up to 10^2 degrees in the mid-band 10^3 rad/s ÷ 10^5 rad/s. Including three modes ($r = 3$) limits the peak error to 10 degrees, and including four modes ($r = 4$) suppresses it to below 1 degree. Below 10 rad/s, all reductions maintain phase shifts under 10^{-3}degrees, indicating excellent preservation of low-frequency dynamics. Above the crossover

frequencies, higher-order modes prove essential to avoid cumulative phase lag. Notably, the $r = 4$ model closely matches the full-order phase response.

Table I compares the MSE of the reduced-model impulse response against the Frobenius-norm reconstruction error of the snapshot ensemble for $r = 1, 2, 3, 4$. While the snapshot error decays monotonically by roughly seven orders of magnitude, confirming that each additional POD mode captures ever finer state-space structures, the time-domain MSE exhibits a non-monotonic dip at $r = 2$, before dramatically falling at $r = 3$ and $r = 4$. This discrepancy indicates that, while subspace projection faithfully reconstructs the raw snapshot matrix, the dynamical weighting of certain modes (e.g., transient peaks) may not be fully align with the singular-value ranking at very low orders. By $r = 4$, the MSE drops by an order of magnitude relative to $r = 3$, demonstrating that retaining four modes suffices to recover both the dominant energy content and the critical transient dynamics of the full-order system.

TABLE I. TIME DOMAIN AND SNAPSHOT RECONSTRUCTION ERRORS FOR POD REDUCTION

Reduction order (r)	MSE of impulse response	Frobenius norm error
1	1.4802×10^{6}	2.4203×10^{-4}
2	1.6421×10^{6}	4.4428×10^{-8}
3	9.6530×10^{5}	1.0271×10^{-11}
4	1.0216×10^{5}	2.0373×10^{-15}

According to the time domain response information in Table II, the full order model's oscillatory step response has a $2.87\ \text{ms}$ rise time and zero overshoot. In contrast, POD reductions dramatically accelerate the dynamics: $r = 1$ achieves a rise time of $0.086\ \text{ms}$, though it inverts the negative settling values, indicating phase distortion. At $r = 2$, the sign remains inverted, and a small overshoot (2.6%) appears. At $r = 3$ and $r = 4$, the polarity recovers; however, large overshoots (27.8% at $r = 3$ and 61.1% at $r = 4$) and undershoots emerge, reflecting an incomplete capture of the higher-order dynamics. While low-order models settle almost instantly ($< 0.3\ \text{ms}$), $r = 4$ exhibits a settling time of $69\ \text{ms}$. This is an order of magnitude slower than the full-order system because slow modes are partially retained without proper balancing. These trends underscore the inherent trade-off in POD reduction: lower-order models yield pronounced speed-up at the expense of fidelity (i.e., amplitude, phase, and settling accuracy), whereas higher-order models ($r \geq 3$) recover amplitude dynamics but introduce excessive oscillations and degraded settling performance.

The overall assessment is as follows: The POD-based reductions exhibit a clear trade-off between model compactness and dynamic fidelity. Very low-order approximations ($r = 1$, $r = 2$) achieve maximal dimensionality reduction, but incur pronounced amplitude and phase distortions in both transient and frequency-domain responses, undermining their reliability for control design. The third-order model restores the dominant dynamics and Bode characteristics to acceptable levels, representing a practical compromise between simplicity and accuracy. The fourth-order model delivers near-full-order performance, virtually indistinguishable in time and frequency-domain metrics, while retaining the computational benefits of reduced dimensionality. Overall, POD proves effective for generating low-order surrogates: moderate-order reductions ($r \geq 3$) strike the best balance, offering substantial complexity reduction without sacrificing essential dynamic behavior, whereas extreme truncations require caution due to their limited fidelity.

TABLE II. STEP RESPONSE CHARACTERISTICS OF FULL ORDER AND POD REDUCED MODELS

Parameter	Full order $n = 5$	Order $r = 4$	Order $r = 3$	Order $r = 2$	Order $r = 1$
Rise time (s)	2.865×10^{-3}	8.612×10^{-5}	9.492×10^{-5}	1.977×10^{-4}	3.991×10^{-4}
Transient time (s)	5.152×10^{-3}	1.534×10^{-4}	3.025×10^{-4}	1.753×10^{-3}	6.867×10^{-2}
Settling time (s)	5.167×10^{-3}	1.534×10^{-4}	3.025×10^{-4}	1.937×10^{-3}	6.957×10^{-2}
Settling min	1.800	–0.121	–0.167	0.139	0.250
Settling max	1.998	–0.109	–0.147	0.196	0.968
Overshoot (%)	0	0	2.595	27.772	61.066
Undershoot (%)	1.159	0	0	87.490	5.271
Peak value	1.998	0.121	0.167	0.196	0.968
Peak time (s)	9.720×10^{-3}	2.870×10^{-4}	2.347×10^{-4}	9.018×10^{-4}	9.828×10^{-4}

IV. CONCLUSION

This study demonstrates that Proper Orthogonal Decomposition (POD) is a robust model-order-reduction technique for high-gain DC-DC converters based on voltage multipliers. By projecting the full-order system onto subspaces spanned by the dominant singular modes, we achieved progressively tighter alignment of transient and frequency-domain behaviors using only a fraction of the original state variables. Notably, the fourth-order approximation reproduced the full-order impulse response and Bode characteristics with negligible error. Meanwhile, the third-order model attained a balance between dimension reduction and dynamic fidelity that is suitable for many control and simulation tasks.

A key insight is the inherent trade-off between compactness and accuracy. First-order and second-order reductions offer extreme computational simplicity, but they suffer from significant amplitude and phase distortions, rendering them unreliable for precision control. In contrast, models of order three and above preserve the essential energy content and modal interactions responsible for the converter's resonant behavior and transient overshoot, without incurring the exponential growth in state-space complexity associated with higher-order topologies.

Looking forward, further research should explore adaptive snapshot strategies to capture nonlinear and load-dependent phenomena more comprehensively, as well as hybrid reduction schemes that integrate POD with parametric or machine learning-based methods to enhance robustness under varying operating conditions. Additionally, embedding reduced-order models within advanced control frameworks, such as model-predictive control or real-time digital twins, promises to unlock new levels of efficiency and reliability in renewable energy and electric vehicle power systems.

ACKNOWLEDGMENT

The authors gratefully acknowledge Thai Nguyen University of Technology, Vietnam, for supporting this work. This research was not affiliated with any funded scientific project.

REFERENCES

[1] S. Ramamurthi and P. Ramasamy, "High step-up DC-DC converter with switched capacitor-coupled inductor and voltage multiplier module," *International Journal of Power Electronics and Drive Systems*, vol. 13, no. 3, pp. 1599–1604, Sep. 2022, https://doi.org/10.11591/ijpeds.v13.i3.pp1599-1604.

[2] R. Beiranvand and S. H. Sangani, "A Family of Interleaved High Step-Up DC–DC Converters by Integrating a Voltage Multiplier and an Active Clamp Circuits," *IEEE Transactions on Power Electronics*, vol. 37, no. 7, pp. 8001–8014, Jul. 2022, https://doi.org/10.1109/TPEL.2022.3141941.

[3] M. Nikbakht, K. Abbaszadeh, S. Abbasian, H. Allahyari, and S. A. Gorji, "An Ultra-Step-Up Quadratic Boost DC–DC Converter Based on Coupled Inductors and Quasi-Resonance Operation," *IEEE Journal of Emerging and Selected Topics in Industrial Electronics*, vol. 4, no. 4, pp. 1096–1109, Oct. 2023, https://doi.org/10.1109/JESTIE.2023.3302706.

[4] O. Asvadi-Kermani, B. Felegari, H. Momeni, S. A. Davari, and J. Rodriguez, "Dynamic Neural-Based Model Predictive Voltage Controller for an Interleaved Boost Converter With Adaptive Constraint Tuning," *IEEE Transactions on Industrial Electronics*, vol. 70, no. 12, pp. 12739–12751, Dec. 2023, https://doi.org/10.1109/TIE.2023.3234138.

[5] A. M. S. S. Andrade, T. M. K. Faistel, A. Toebe, R. A. Guisso, and M. M. da Silva, "High step-up active switched coupled inductor DC-DC converter with voltage multiplier," *International Journal of Circuit Theory and Applications*, vol. 50, no. 11, pp. 3911–3925, Nov. 2022, https://doi.org/10.1002/cta.3369.

[6] K.-L. Tsao, C.-I. Liu, K.-K. Shyu, P.-L. Lee, and S.-C. Huang, "High Efficient Step-up DC-DC Converter With Zero Current Switching And Voltage Multiplier Cell," in *2024 International Automatic Control Conference*, Taoyuan, Taiwan, 2024, pp. 1–6, https://doi.org/10.1109/CACS63404.2024.10773164.

[7] P. H. Feretti, F. L. Tofoli, and E. R. Ribeiro, "Family of Non-Isolated High Step-Up DC–DC Converters Based on the Multi-State Switching Cell," *IEEE Journal of Emerging and Selected Topics in Power Electronics*, vol. 10, no. 5, pp. 5882–5893, Oct. 2022, https://doi.org/10.1109/JESTPE.2022.3160280.

[8] Y. Xu *et al.*, "Y-Source Coupled Inductor Based High Voltage Gain DC–DC Converter With Zero Input Current Ripple," *IEEE Journal of Emerging and Selected Topics in Power Electronics*, vol. 13, no. 1, pp. 199–213, Feb. 2025, https://doi.org/10.1109/JESTPE.2024.3496879.

[9] R. K. Patnaik, A. Saravanan, K. Patidar, C. Jeeva, E. S. Prasad, and G. Dharmaraj, "Transformerless high step-up DC–DC converter with voltage multiplier concept," *AIP Conference Proceedings*, vol. 2690, no. 1, Mar. 2023, Art. no. 020043, https://doi.org/10.1063/5.0120163.

[10] T. C. Salvador, F. L. Tofoli, D. de Souza Oliveira Júnior, and E. R. Ribeiro, "Nonisolated high step-up DC-DC interleaved SEPIC converter based on voltage multiplier cells," *International Journal of Circuit Theory and Applications*, vol. 50, no. 8, pp. 2735–2758, Aug. 2022, https://doi.org/10.1002/cta.3307.

[11] E. Sreelatha, A. Pandian, P. Sarala, and C. R. Reddy, "Design of Symmetrical Voltage Multiplier High Gain Interleaved DC to DC Converter for Photovoltaic Applications," *Engineering, Technology & Applied Science Research*, vol. 14, no. 3, pp. 14525–14532, Jun. 2024, https://doi.org/10.48084/etasr.7135.

[12] A. B. Rehiara, Y. Rumengan, P. Sarungallo, and Hendri, "Three Leg Inverter Control based on Laguerre Model Predictive Controller," *Engineering, Technology & Applied Science Research*, vol. 14, no. 6, pp. 17591–17598, Dec. 2024, https://doi.org/10.48084/etasr.8385.

[13] S. Karike, K. N. Raju, and S. R. Donepudi, "Efficient On-Board Charger to Improve the Life Time of Electric Vehicle Battery," *Engineering, Technology & Applied Science Research*, vol. 14, no. 3, pp. 14451–14457, Jun. 2024, https://doi.org/10.48084/etasr.7111.

[14] Y.-S. Lee, K.-M. Choo, C.-H. Lee, C.-G. An, J. Yi, and C.-Y. Won, "Common-Mode Voltage Reduction Method Based on Variable Sampling Frequency Finite Control Set-Model Predictive Control for PMSM Drive Systems," *Energies*, vol. 17, no. 6, Mar. 2024, Art. no. 1443, https://doi.org/10.3390/en17061443.

[15] G. Li and S. W. Or, "Multi-agent deep reinforcement learning-based multi-time scale energy management of urban rail traction networks with distributed photovoltaic–regenerative braking hybrid energy storage systems," *Journal of Cleaner Production*, vol. 466, Aug. 2024, Art. no. 142842, https://doi.org/10.1016/j.jclepro.2024.142842.

[16] K. Fettah *et al.*, "Optimal integration of photovoltaic sources and capacitor banks considering irradiance, temperature, and load changes in electric distribution system," *Scientific Reports*, vol. 15, no. 1, Jan. 2025, Art. no. 2670, https://doi.org/10.1038/s41598-025-85484-3.

[17] F. Dakheel and M. Çevik, "Optimizing Smart Grid Load Forecasting via a Hybrid Long Short-Term Memory-XGBoost Framework: Enhancing Accuracy, Robustness, and Energy Management," *Energies*, vol. 18, no. 11, Jun. 2025, Art. no. 2842, https://doi.org/10.3390/en18112842.

[18] M. Rizwan, S. A. Khan, M. R. Khan, and A. A. Khan, "Experimental and statistical investigation on the dielectric breakdown of magneto nanofluids for power applications," *Journal of Materials Science: Materials in Engineering*, vol. 19, no. 1, Jul. 2024, Art. no. 5, https://doi.org/10.1186/s40712-024-00144-0.

[19] Y. Wan, J. Zhao, and G. M. Dimirovski, "Robust adaptive control for a single-machine infinite-bus power system with an SVC," *Control Engineering Practice*, vol. 30, pp. 132–139, Sep. 2014, https://doi.org/10.1016/j.conengprac.2013.06.020.

[20] Q. Zhang and G. Li, "Experimental Study on a Semi-Active Battery-Supercapacitor Hybrid Energy Storage System for Electric Vehicle Application," *IEEE Transactions on Power Electronics*, vol. 35, no. 1, pp. 1014–1021, Jan. 2020, https://doi.org/10.1109/TPEL.2019.2912425.

[21] J. L. Nicolini, F. L. Teixeira, and R. J. Burkholder, "Reduced-Order Mode Discovery in Arbitrary Cavities via Proper Orthogonal Decomposition," in *2023 IEEE International Symposium on Antennas and Propagation and USNC-URSI Radio Science Meeting*, Portland, OR, USA, 2023, pp. 837–838, https://doi.org/10.1109/USNC-URSI52151.2023.10238003.

[22] T. Li, T. Pan, X. Zhou, K. Zhang, and J. Yao, "Non-Intrusive Reduced-Order Modeling Based on Parametrized Proper Orthogonal Decomposition," *Energies*, vol. 17, no. 1, Jan. 2024, Art. no. 146, https://doi.org/10.3390/en17010146.

[23] R. Torchio, A. Zanco, F. Lucchini, P. Alotto, and S. Grivet-Talocia, "Mixed Proper Orthogonal Decomposition with Harmonic Approximation for Parameterized Order Reduction of Electromagnetic Models," in *2022 International Symposium on Electromagnetic Compatibility – EMC Europe*, Gothenburg, Sweden, 2022, pp. 349–354, https://doi.org/10.1109/EMCEurope51680.2022.9901091.

[24] Y. Tan, J. Jiang, C. Huang, and H. Ishikuro, "Orthogonal Decomposition Based Digital Controller Design for Hybrid Converter," in *2024 IEEE 67th International Midwest Symposium on Circuits and Systems*, Springfield, MA, USA, 2024, pp. 1378–1382, https://doi.org/10.1109/MWSCAS60917.2024.10658813.

[25] S. Ritzert, D. Macek, J.-W. Simon, and S. Reese, "An adaptive model order reduction technique for parameter-dependent modular structures,"

Computational Mechanics, vol. 73, no. 5, pp. 1147–1163, May 2024, https://doi.org/10.1007/s00466-023-02404-w.

[26] R. Abadía-Heredia, M. López-Martín, B. Carro, J. I. Arribas, J. M. Pérez, and S. Le Clainche, "A predictive hybrid reduced order model based on proper orthogonal decomposition combined with deep learning architectures," *Expert Systems with Applications*, vol. 187, Jan. 2022, Art. no. 115910, https://doi.org/10.1016/j.eswa.2021.115910.

[27] D. Thaler, M. D. Shields, B. Markert, and F. Bamer, "Model order reduction in subset simulations using the proper orthogonal decomposition," *PAMM*, vol. 23, no. 4, Dec. 2023, Art. no. e202300053, https://doi.org/10.1002/pamm.202300053.

[28] Z. Wang, G. Zhang, T. Sun, and H. Huang, "Information sharing-based multivariate proper orthogonal decomposition," *Physics of Fluids*, vol. 35, no. 10, Oct. 2023, Art. no. 104108, https://doi.org/10.1063/5.0169994.

[29] A. Bandera, S. Fernández-García, M. Gómez-Mármol, and A. Vidal, "Automatic Proper Orthogonal Block Decomposition method for network dynamical systems with multiple timescales," *Communications in Nonlinear Science and Numerical Simulation*, vol. 131, Apr. 2024, Art. no. 107844, https://doi.org/10.1016/j.cnsns.2024.107844.

[30] Annaneya, V. P. Meena, A. V. Waghmare, and V. P. Singh, "Reduced-order Modelling of Level-Up DC-DC Converter Using TLBO Algorithm," in *2023 IEEE 3rd International Conference on Sustainable Energy and Future Electric Transportation*, Bhubaneswar, India, 2023, pp. 1–6, https://doi.org/10.1109/SeFeT57834.2023.10245797.